BIOCHEMISTRY
including biophysical chemistry & molecular biology

Article

pubs.acs.org/biochemistry

Further Studies on the Role of Water in R67 Dihydrofolate Reductase

Mary Jane Timson,[†] Michael R. Duff, Jr.,[†] Greyson Dickey,[†] Arnold M. Saxton,[‡] José I. Reyes-De-Corcuera,[§] and Elizabeth E. Howell*,[†]

[†]Department of Biochemistry and Cellular and Molecular Biology, University of Tennessee, Knoxville, Tennessee 37996-0840, United States

[‡]Department of Animal Science, University of Tennessee, Knoxville, Tennessee 37996, United States

[§]Citrus Research and Education Center, Institute of Food and Agricultural Sciences, University of Florida, 700 Experiment Station Road, Lake Alfred, Florida 33850-2299, United States

Supporting Information

ABSTRACT: Previous osmotic pressure studies of two nonhomologous dihydrofolate reductase (DHFR) enzymes found tighter binding of the nicotinamide adenine dinucleotide phosphate cofactor upon addition of neutral osmolytes. This result is consistent with water release accompanying binding. In contrast, osmotic stress studies found weaker binding of the dihydrofolate (DHF) substrate for both type I and type II DHFRs in the presence of osmolytes; this observation can be explained if dihydrofolate interacts with osmolytes and shifts the equilibrium from the enzyme-bound state toward the unbound substrate. Nuclear magnetic resonance experiments support this hypothesis, finding that osmolytes interact with dihydrofolate. To consider binding without added osmolytes, a high-pressure approach was used. In this study, the type II enzyme, R67 DHFR, was subjected to high hydrostatic pressure (HHP). Both enzyme activity and fluorescence measurements find the protein tolerates pressures up to 200 MPa. Binding of the cofactor to R67 DHFR weakens with increasing pressure, and a positive association volume of 11.4 ± 0.5 cm^3/mol was measured. Additionally, an activation volume of 3.3 ± 0.5 cm^3/mol describing $k_{cat}/K_{m(DHF)}$ was determined from progress curve analysis. Results from these HHP experiments suggest water release accompanies binding of both the cofactor and DHF to R67 DHFR. In an additional set of experiments, isothermal titration calorimetry studies in H_2O and D_2O find that water reorganization dominates the enthalpy associated with binding of DHF to R67 DHFR·$NADP^+$, while no obvious effects occur for cofactor binding. The combined results indicate that water plays an active role in ligand binding to R67 DHFR.

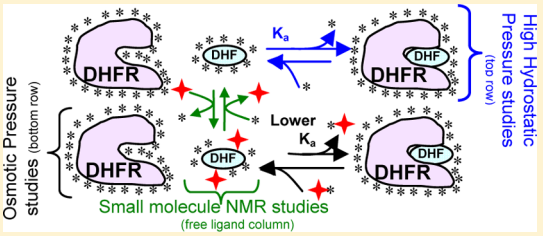

Association of protein to protein, ligand to receptor, substrate to enzyme, or a drug to its target is critical to macromolecular function. Binding encompasses two events, desolvation and association. Although the parameters involved in association are reasonably well understood, the behavior of water remains unclear. This is one of the difficulties in being able to design drugs or predict binding affinity.[1−3] While water is ubiquitous, it is usually ignored when binding is considered. In vitro experiments often use water at high concentrations, while in vivo, the concentration of water is decreased because of the presence of high concentrations of molecules in the cellular milieu.

Two approaches to studying the role of water are osmotic pressure and high hydrostatic pressure (HHP). Addition of small molecules, or osmolytes, decreases the water concentration, while pressurization decreases the volume. An increased pressure also results in penetration of water into the protein matrix;[4,5] thus, HHP typically counteracts the effects of osmotic pressure.[6−8] For example, osmotic pressure increases the star activity (relaxation or alteration of the specificity) of the restriction endonuclease, EcoRI.[9] However, increasing HHP restores the ability of EcoRI to correctly discriminate between normal and star sequences, presumably by restoration of the hydration shell in the enzyme.

We have previously studied the role of water in ligand binding to R67 dihydrofolate reductase (DHFR) using an osmotic pressure approach and found tighter binding of cofactor and weaker binding of substrate. These results are consistent with water release upon cofactor binding and "water uptake" upon substrate binding.[10] "Water uptake" could occur if additional water molecules are required to mediate the ligand−protein interaction or if a conformational change occurred in the protein such that an increase in surface area occurred upon binding.[11−13] More recently, we have monitored binding of DHF to a second DHFR, the nonhomologous chromosomal *Escherichia coli* DHFR, in the presence of osmolytes and found similar numbers of water molecules "taken up" upon DHF binding.[14] Because these two DHFRs have entirely different folds, the similarity of these water uptake results implicates association of osmolytes with DHF (i.e., a preferential interaction model). Indeed, a recent nuclear

Received: November 16, 2012
Revised: February 21, 2013
Published: March 4, 2013

magnetic resonance (NMR) study indicates that osmolytes interact with folate derivatives in solution.[15] A model describing this situation is given in Figure 1. When a ligand binds to a

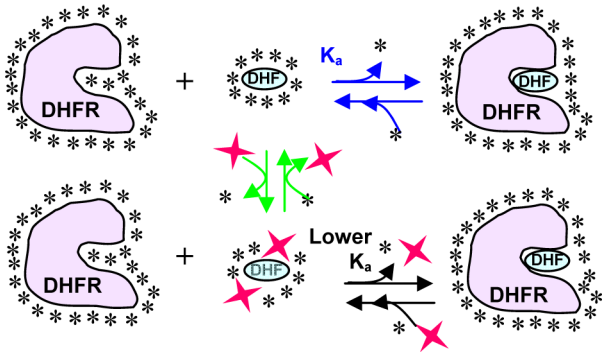

Figure 1. Cartoon depicting preferential interaction of osmolytes with free DHF (blue circle). In the absence of osmolytes, water (asterisks) is released when DHF binds tightly to its target DHFR. Added osmolytes (red star) interact weakly with DHF.[10] For DHF to bind to the enzyme, both osmolytes and water must be released. Osmolytes that bind more tightly than water would have larger effects on the DHF K_a, while the more weakly bound osmolytes would have smaller effects. (Note that this model does not exclude the possible binding of osmolytes to the enzyme, which could describe the differing effects of osmolytes on the binding of $NADP^+$ to EcDHFR.)[14] In this study, we use high hydrostatic pressure to examine the top row of the model (blue equilibrium arrows). We have previously used NMR to observe interactions between folate and osmolytes (middle column, green equilibrium arrows).[15]

macromolecule, water molecules are displaced from the hydration layer, increasing the number of contacts between the two molecules. Interaction between osmolytes and DHF will shift the substrate binding equilibrium away from the bound state (bottom row of Figure 1). To investigate the role of water upon binding of DHF to DHFR without the interference of osmolytes (top row of Figure 1), high-hydrostatic pressure studies can be used. An increased level of hydration at higher pressures predicts binding of DHF to R67 DHFR will be facilitated if water uptake does indeed occur and changes in enzyme conformation do not result in the obstruction of the active site. If, however, the osmolytes are interacting with free DHF, then the HHP results should instead correlate with changes in the accessible surface area (ASA) upon complex formation.

Another approach to modulating water properties is to substitute D_2O for H_2O in binding experiments. D_2O has properties different from those of normal water, one of them being a roughly 10% change in the enthalpy for a hydrogen bond in D_2O versus H_2O. Using this relationship, Chervenak and Toone examined the contribution of water reorganization to ligand binding.[16] For binding of carbohydrates to lectins, they predicted solvent reorganization contributed from 25 to 100% of the overall enthalpy. We use this approach to continue parsing out the role of water in binding of ligands to R67 DHFR.

In these studies, we use the model protein R67 DHFR as it has been well studied.[17−20] This enzyme catalyzes the reduction of dihydrofolate (DHF) to tetrahydrofolate using nicotinamide adenine dinucleotide phosphate (NADPH) as a cofactor. R67 was identified in the 1970s as a resistance protein that confers trimethoprim (TMP) resistance upon host bacteria.[21,22] R67 DHFR provides resistance to TMP at concentrations that inhibit the drug target, chromosomal DHFR. R67 DHFR is a homotetramer (Figure 2), and its single active site pore

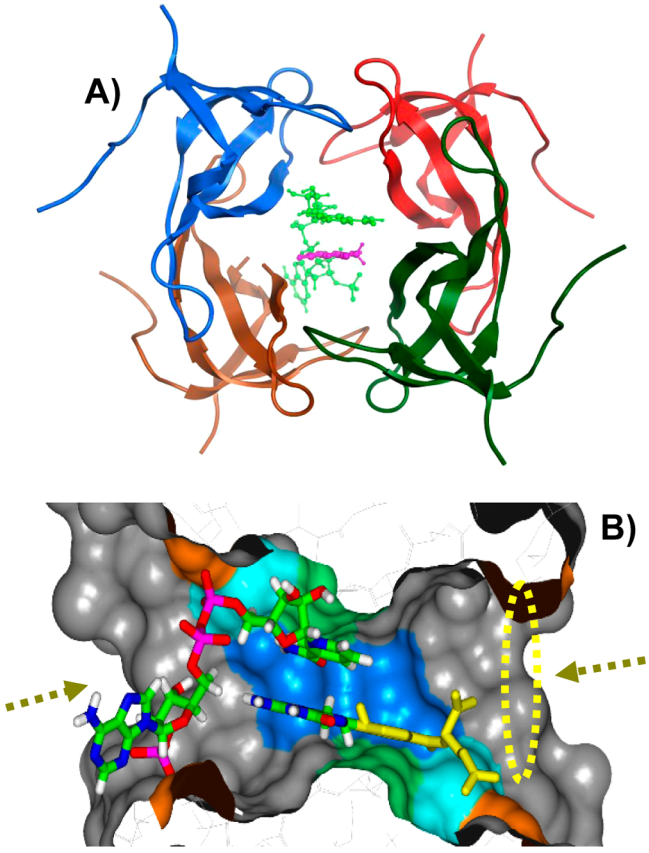

Figure 2. (A) Structure of the R67 DHFR tetramer (Protein Data Bank entry 2RH2).[17] The top view shows each different monomer in a different color. The central pore is the active site, and bound dihydrofolate and $NADP^+$ are colored magenta and green, respectively. The *p*-amino-benzoyl-glutamate tail of DHF is disordered. (B) This panel is related to panel a by a 90° rotation around the *y*-axis, followed by slicing through the structure to show the pore. A Connolly surface displays the positions of key residues: K32 (orange), I68 (blue), Q67 (green), and Y69 (cyan). Arrows on opposite sides of the pore indicate entry of the ligands. In this ternary complex structure, $NADP^+$ enters from the left and DHF from the right;[17] however, binding at symmetry-related sites can also occur. The color code for the atoms is as follows: carbon, green; nitrogen, blue; oxygen, red; phosphorus, magenta; hydrogen, white. The pteridine ring of folate is fixed near the center of the pore; however, the *p*-amino-benzoyl-glutamate tail is disordered. One potential tail conformer was built in the structure (colored yellow). Alternate tail positions are suggested by the circular arrow and supported by disorder in crystal structures,[17,23] NMR analysis,[50] and molecular dynamics simulations.[51]

possesses 222 symmetry.[23] Because of this symmetry, it utilizes a promiscuous binding surface that can accommodate either NADPH or DHF. Either two NADPH molecules, two folate·DHF molecules, or one DHF and one NADPH bind to R67, with the latter complex being the productive catalytic species.[19] Binding is funneled toward the productive enzyme·DHF·NADPH complex by interligand cooperativity patterns with a preference for NADPH to bind first. Our previous steady state kinetics, isothermal titration calorimetry (ITC) binding studies, and genetic selections in the presence of sorbitol have found effects of water and osmolytes on R67

dx.doi.org/10.1021/bi301544k | *Biochemistry* 2013, 52, 2118−2127

DHFR function.[10] The study presented here further explores the role of water, particularly in ligand binding.

MATERIALS AND METHODS

Protein Purification. R67 DHFR was purified as previously described.[24] Briefly, ammonium sulfate precipitation, ion-exchange, and size-exclusion column chromatography steps were used to purify the protein to homogeneity. Purified samples were dialyzed against distilled, deionized H_2O and then lyophilized. Protein concentrations were determined with a bicinchoninic acid assay (Pierce).

High-Hydrostatic Pressure Measurements. The HHP system consists of a high-pressure reactor (model U103), a high-pressure micropump (model MP5), and a pump controller (MP5 micropump control unit), all from Unipress Equipment (Warsaw, Poland). The temperature of the reactor is controlled by a water jacket connected to a water bath. Computer programs written in LabVIEW version 8.0 and a data acquisition board (DAQ Card 6062E) from National Instruments allow collection of temperature and pressure data. This system has been previously described.[25]

The U103 optical vessel has three optical (sapphire) windows, allowing either absorbance or fluorescence to be monitored via optical fibers. Samples were loaded in cylindrical, quartz cuvettes (0.7 cm path length, GE 214). The light source was a DH-2000 UV−vis−NIR system from Mikropack possessing deuterium and halogen lamps. Use of an HR4000CG-UV-NR high-resolution spectrometer for absorbance measurements, a USB-4000 spectrometer for fluorescence, and OOIBase32 software (Ocean Optics, Inc., Dunedin, FL) allowed visualization and collection of spectral information. Output files were exported into Microsoft Excel for analysis. Experiments were performed between 0.1 and 500 MPa.

Protein Fluorescence at HHP. Using the HHP system described above, the intrinsic fluorescence of 10 μM R67 DHFR was monitored in 89 mM Tris plus 11 mM KH_2PO_4 (pH 7.0). This buffer maintains a constant pH as pressure is increased.[26] All HHP studies were performed in this buffer.

The deuterium and halogen lamps provide a broad excitation band. While filters could be used to provide more specificity for excitation of tryptophan residues, they substantially decrease the signal intensity and were not used. Control scans of buffer were obtained and subtracted from the protein scans.

Fluorescence Quenching at HHP. Binding of NADPH to 10 μM R67 DHFR was monitored by fluorescence as described above. Control scans of the cofactor and buffer were obtained and subtracted from those of the protein plus cofactor mixture. The fluorescence intensities at 340 nm were fit to

$$\mathrm{Fl}_{obs} = F_0 - 0.5F_0\left[P_{tot} + K_d + L_{tot} - \sqrt{(P_{tot} + K_d + L_{tot})^2 - 4P_{tot}L_{tot}}\right] \quad (1)$$

where Fl_{obs} is the observed fluorescence, L_{tot} is the total ligand concentration, and P_{tot}, K_d, and F_0 describe the number of enzyme binding sites, the dissociation constant, and the fluorescence yield per unit concentration of enzyme, respectively.[27]

To allow ready comparison, data were normalized according to

$$F_{app} = \frac{\mathrm{Fl}_{apo} - \mathrm{Fl}_{obs}}{\mathrm{Fl}_{apo} - \mathrm{Fl}_{bound}} \quad (2)$$

where F_{app} is a fractional value between 0 and 1 and Fl_{obs}, Fl_{apo}, and Fl_{bound} are the fluorescence values associated with the observed, apo, and ligand-bound forms, respectively.

Kinetics at HHP. DHF was prepared by reduction of folate as described by Blakley.[28] NADPH was obtained from Alexis Biochemicals. Concentrations of DHF and NADPH were measured using their extinction coefficients of 28000 M^{-1} cm^{-1} at 280 nm[28] and 6230 M^{-1} cm^{-1} at 340 nm, respectively.[29] The extinction coefficient for the reduction of DHF and NADPH by DHFR is 12300 M^{-1} cm^{-1} at 340 nm.[30]

Steady state kinetics were performed by mixing the various solutions at room pressure and inserting the cuvette into the optical vessel. This process took approximately 1 min. Reaching the desired pressure took an additional 0.5−1 min. Rates were then collected for typically 10 min. Concentrations of the cofactor (70−100 μM) and DHF (70−120 μM) that were saturating at ambient pressure were utilized (the K_m values at ambient pressure are 2.5 and 5.8 μM, respectively).[24] Data were typically fit from 2 to 8 min. Rates were usually constant for up to 8−10 min.

Progress curve analysis on R67 DHFR was performed using a method similar to that of Gekko et al.[31] Reaction solutions were prepared by mixing a saturating concentration of NADPH (165 μM) with DHF (65 μM) and R67 DHFR (450 nM) at ambient pressure. The solution was then quickly transferred to the cuvette in the pressure chamber equilibrated with a water bath at 30 °C, which was then pressurized. The time from sample preparation to starting the kinetic scan was approximately 2 min. The reaction was monitored at 340 nm until all the DHF was consumed (7−10 min). MATLAB (version r2012a, MathWorks, Inc.) was used to fit the data to the integrated Michaelis−Menten equation.[31]

Isothermal Titration Calorimetry. The observed enthalpy, ΔH_{obs}, can be expressed as

$$\Delta H_{obs} = \Delta H_{intrinsic} + \Delta H_{solvent} \quad (3)$$

where $\Delta H_{intrinsic}$ arises from protein−ligand interactions and $\Delta H_{solvent}$ from water reorganization. The latter term involves desolvation events as well as changes in solvent−solvent interactions. To parse out the contribution of $\Delta H_{solvent}$ to ΔH_{obs}, we performed binding in D_2O as described by Chervenak and Toone.[16]

Affinities, stoichiometries, and ΔH values associated with binding were determined using ITC as previously described.[19] At least two replicate titrations at 25 °C were performed using a VP-ITC microcalorimeter from MicroCal. DHFR concentrations ranged from 99 to 115 μM; the buffer consisted of 10 mM Tris and 1 mM EDTA buffer (TE) (pH 7.5) with 102 mM NaCl. Care was taken to match the pH of all the solutions. A 1:5 ratio of enzyme to $NADP^+$ was used to monitor DHF ternary complex formation. The "c value" ($=[\mathrm{protein}]_{total}/K_d$) ranged from 1 to 40, within the suggested range of 1−1000.[32] For the NADPH binary complex, additional data sets were collected, where low concentrations of cofactor (3 μL injections of 0.37−0.63 mM) were injected into 103−106 μM R67 DHFR. For these experiments, all the cofactor binds, resulting in heats of injection that are reasonably constant. This allows calculation of molar enthalpy values (after subtraction of a heat of dilution term) without the use of a model.[33]

dx.doi.org/10.1021/bi301544k | Biochemistry 2013, 52, 2118−2127

D_2O (99.9 atom % D), DCl, NaOD, and deuterated Tris were obtained from Cambridge Isotopes (Andover, MA). For measurements in D_2O, lyophilized protein, folate, NADPH, $NADP^+$, and EDTA went through a cycle of reconstitution in D_2O and equilibration (1 h for small ligands and 3 days for protein), followed by lyophilization. This cycle was repeated. For the ITC measurements, the deuterated protein and ligand were reconstituted in deuterated TE buffer with salt. All solutions were titrated to pH 7.5. Uncorrected pH-meter readings were used as typically the 0.4 pH meter offset is similar to any shifts in pK_a values.[34,35] Because the stability of DHF is limited once it is synthesized, it was frozen and stored as a suspension in 5 mM HCl. In these experiments, the DHF pellet was washed twice with 5 mM DCl prior to use.

Origin version 7 and SEDPHAT[36] were used to analyze the ITC data. Export of Origin data into SEDPHAT allows global fitting of replicate data sets. Errors were calculated using the Monte Carlo for the nonlinear regression option in SEDPHAT. Ternary complex data were fit to a single-site model. Folate binary data were fit to a two-site model, which yields macroscopic binding constants. The relationships between macroscopic and microscopic constants are $K_{1macro} = k_{1micro}/2$ and $K_{2macro} = 2k_{2micro}$ for the first and second sites, respectively.

RESULTS

Effects of HHP on Apoprotein Fluorescence. To determine the pressure range where pressure starts to alter the R67 DHFR oligomerization state and/or structure, we monitored the intrinsic fluorescence of R67 DHFR as a function of increasing pressure. Figure 3 plots the emission spectra as pressure is increased in 25 MPa increments from atmospheric pressure to 500 MPa. While there is a decrease in the overall fluorescence intensities, a red shift in the emission curves is observed only at high pressures. A plot of fluorescence intensity at 360 nm reveals the beginning of the red shift near 300 MPa.

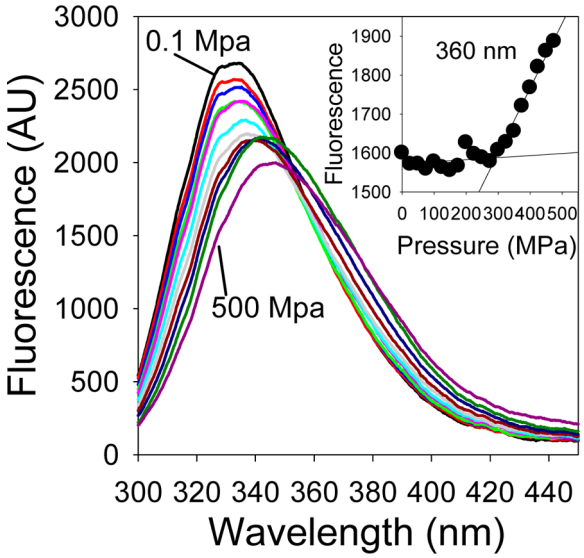

Figure 3. Fluorescence emission spectra of 10 μM R67 DHFR in 89 mM Tris plus 11 mM KH_2PO_4 (pH 7.0) at increasing pressures. The initial spectrum was recorded at room pressure. The pressure was then increased by 25 MPa and the spectrum re-recorded. This process was repeated until the pressure reached 500 MPa. For the sake of clarity, emission spectra are presented only every 50 MPa. The spectra are for 0.1 (black), 50 (red), 100 (blue), 150 (green), 200 (magenta), 250 (cyan), 300 (gray), 350 (dark red), 400 (dark blue), 450 (dark green), and 500 MPa (dark magenta). A red shift is observed, and the inset plots the fluorescence intensity at 360 nm. A clear shift occurs at ≥300 MPa.

Effects of HHP on k_{cat}. As shown in Figure S1 of the Supporting Information, the effect of HHP on k_{cat} was measured using levels of substrate and cofactor that were greater than 10 times the K_m values at ambient pressures. A minimal effect on k_{cat} was observed from room pressure to 200 MPa, while above this pressure, k_{cat} decreases. Combined with the effects of HHP on apoprotein fluorescence described above, these two data sets define a range of pressures from 0.1 to 200 MPa that appear to have minimal effects on protein structure and activity. This is also the pressure range most often used to study enzyme function,[31,37,38] as hydrostatic pressure tends to dissociate oligomeric protein complexes around 100−200 MPa and typically induces protein unfolding above 400 MPa.[4,9]

To determine if HHP effects on k_{cat} are reversible, a steady state rate at saturating DHF and NADPH concentrations was first monitored at room pressure. Then a pressure of 500 MPa was applied for at least 2 min, followed by the release of pressure. Figure S2 of the Supporting Information shows the absorbance trace. The final rate was ∼70% of the initial rate, consistent with recovery of most of the activity. The difference may be due to either a slow rate of activity recovery or the loss of k_{cat} conditions after 7 min.

Effects of HHP on NADPH Binding. Cofactor binding was monitored by quenching of protein fluorescence. A sample series of emission curves at 100 MPa is shown in Figure 4A. Binding constants were calculated, and weaker binding is observed with an increasing pressure. Figure 4B plots ln K_a versus pressure up to 250 MPa. The slope of this plot yields the change in volume for association of NADPH with R67 DHFR, which is 11.4 ± 0.5 cm^3/mol (see Table 1). These results indicate a pressure-disfavored volume expansion upon cofactor binding.

Effects of HHP on Substrate Binding. We were unable to directly monitor binding of DHF/folate by fluorescence quenching as two molecules of DHF bind per R67 active site, with positive cooperativity and K_d values of 125 and 8.8 μM.[19] If we saturate the sample with $NADP^+$ (stoichiometry of 1) and then add DHF, the protein fluorescence has already been greatly quenched; thus, it is difficult to monitor an additional signal loss. To gain information about HHP effects on DHF capture, we turned to measurement of k_{cat} and K_m using progress curve analysis.

Progress curves were measured for R67 DHFR where the DHF concentration was limiting. While pressure should weaken binding of NADPH, the decrease in K_a is known (Figure 4) and the NADPH concentration is almost 30 times higher than its K_d value at 175 MPa. A typical progress curve at 175 MPa and its fit are provided in Figure S3 of the Supporting Information. Increases in both k_{cat} (from 0.5 to 2.0 s^{-1})[a] and $K_{m(DHF)}$ (from 14 to 68 μM) occurred when the pressure was increased from 0.1 to 175 MPa. The value for k_{cat} at ambient pressure is comparable to previous values measured by steady state kinetics; however, the $K_{m(DHF)}$ is more than 2-fold higher.[24] Gekko et al. noted similarly high K_m values from progress curve analysis of the EcDHFR reaction.[31] They suggested the increased K_m values could be due to product inhibition and/or some contribution from a reverse reaction. Figure 5 plots ln k_{cat} and ln $k_{cat}/K_{m(DHF)}$ versus increasing HHP.

dx.doi.org/10.1021/bi301544k | Biochemistry 2013, 52, 2118−2127

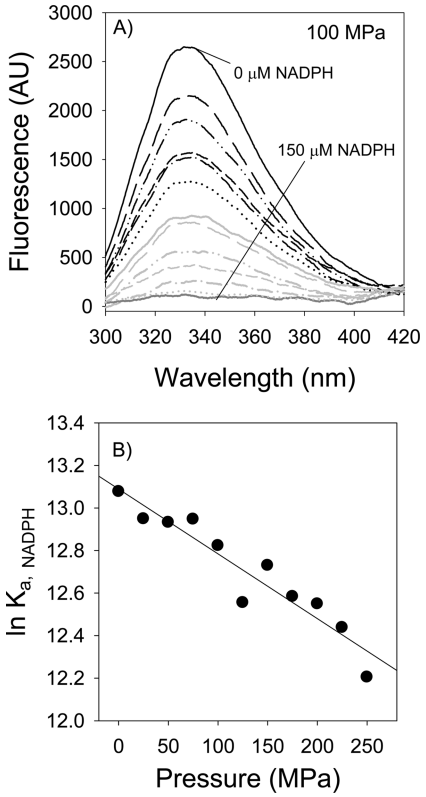

Figure 4. Plots describing binding of NADPH to R67 DHFR. (A) Quenching of protein fluorescence at 100 MPa upon addition of increasing concentrations of NADPH: 0 (solid line), 2 (long dash line), 4 (dash−dot−dot line), 6 (short dash line), 8 (dot−dash line), 10 (dotted line), 15 (solid gray line), 20 (long gray dash line), 30 (gray dash−dot−dot line), 50 (gray short dash line), 75 (gray dot−dash line), 100 (gray dotted line), and 150 μM (dark gray line). (B) Plots of ln K_a vs HHP. The slope can be converted into a volume change for association of cofactor with R67; this value is 11.4 ± 0.5 cm^3/mol.

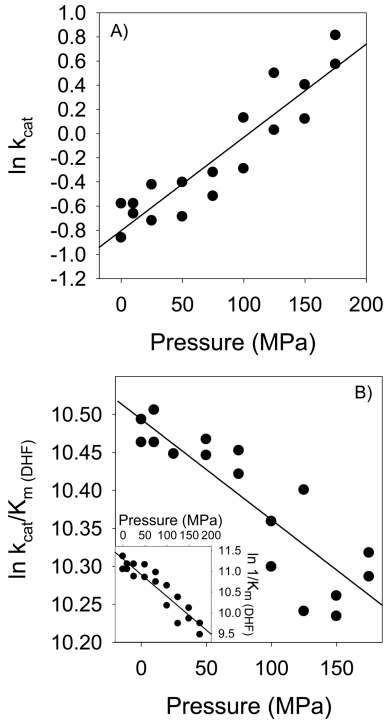

Figure 5. Plots of ln k_{cat} (A) and ln k_{cat}/K_m (B) for R67 DHFR vs HHP. Rates were determined using progress curve analysis for DHFR (450 nM) with a limiting concentration of DHF (65 μM) and an excess concentration of NADPH (165 μM). Activation volumes are listed in Table 1. A plot of ln $1/K_m$ is shown as an inset in panel B.

While k_{cat} increases at high HHP, indicating pressure favors a smaller reaction volume, $k_{cat}/K_{m(DHF)}$ decreases, indicating pressure disfavors this rate.

An activation volume, defined as a change in molar volume associated with formation of the transition state from the ternary E·NADPH·DHF complex, can be determined from a plot of ln k_{cat} versus pressure according to Eyring's equation. The slope equals $-\Delta V/R_pT$, where V is volume, R_p is the universal gas constant (8.314 cm^3 MPa mol^{-1} K^{-1}), and T is temperature.[39] An activation volume of −19.4 ± 2.0 cm^3/mol was calculated from the data in Figure 5 for the 0.1−175 MPa range (see Table 1). Negative activation volumes indicate that the rate-limiting step is accompanied by a volume decrease. An activation volume of 3.3 ± 0.5 cm^3/mol was also calculated for $k_{cat}/K_{m(DHF)}$. This activation value describes the capture of DHF by R67 DHFR·NADPH and subsequent transition state formation. A plot of $1/K_{m(DHF)}$ versus HHP was additionally constructed (see the inset of Figure 5). If $K_{m(DHF)}$ equals $K_{d(DHF)}$, a potential association volume for binding of DHF to R67·NADPH can be calculated as 22.8 ± 2.3 cm^3/mol. Previous kinetic and ITC results have indicated that K_m is a good approximation of K_d for DHF binding to R67 DHFR, at least at ambient pressure.[10,40]

We have additionally monitored $k_{cat}/K_{m(DHF)}$ rates for a Y69L mutant of R67 DHFR using steady state kinetics. These data are given in Figure S4 of the Supporting Information, and a positive activation volume was also obtained.

Pressure perturbation calorimetry (PPC) was also used to explore the role of pressure in binding of substrate to R67 DHFR (see the Supporting Information for experimental details and results). PPC measures the change in heat of a solution upon the application of pressure.[41] The change in heat is proportional to the molar expansivity of the solutes, such as protein or the protein−ligand complex.[42] Subtracting the molar expansivity of the free protein and free ligand from that of the protein−ligand complex has been proposed to allow calculation of the number of waters released upon ligand binding.[43]

Table 1. Association and Activation Volumes for Binding and Catalytic Events in R67 DHFR (89 mM Tris plus 11 mM KH_2PO_4, pH 7.0, 30 °C, and 0.1−200 MPa) and EcDHFR (20 mM Tris-HCl, 0.1 mM EDTA, and 0.1 mM dithiothreitol, pH 7.0, 25 °C, and 50−200 MPa) As Measured by HHP[31]

protein	activation volume for k_{cat} (cm^3/mol)	association volume for $K_{a(NADPH)}$ (cm^3/mol)	association volume for $K_{a(folate)}$ (cm^3/mol)	activation volume for $k_{cat}/K_{m(DHF)}$ (cm^3/mol)	association volume for $1/K_{m(DHF)}$ (cm^3/mol)
R67 DHFR	−19.4 ± 2.0	11.4 ± 0.5	–	3.3 ± 0.5	22.8 ± 2.3
EcDHFR[a]	7.8 ± 0.6[a]	37.5 ± 2[a]	7.3 ± 0.4[a]		–

[a]Values from ref 31.

dx.doi.org/10.1021/bi301544k | Biochemistry 2013, 52, 2118−2127

Table 2. Thermodynamic Parameters Associated with Binary and Ternary Complex Formation, TE Buffer, pH 7.5, 25 °C, and an Ionic Strength of 0.11[a]

complex	solvent	K_d (μM)	ΔG (kcal/mol)	ΔH_{obs} (kcal/mol)	$T\Delta S$ (kcal/mol)	n	$\Delta\Delta H$ (kcal/mol) = $\Delta H_{H_2O} - \Delta H_{D_2O}$
NADPH−R67 DHFR	H_2O	−	−	−6.08 ± 0.4	−	−	within error
NADPH−R67 DHFR	D_2O	−	−	−6.06 ± 0.3	−	−	
folate−R67 DHFR	H_2O (first site)	152 ± 15	−5.20	−2.73 ± 0.17	2.47	0.90 ± 0.02	2.7 (first site)
	H_2O (second site)	75.7 ± 18	−5.62	−9.31 ± 0.34	−3.69		
folate−R67 DHFR	D_2O (first site)	144 ± 6	−5.24	−5.43 ± 0.21	−0.19	0.78 ± 0.01	−1.06 (second site)
	D_2O (second site)	41.0 ± 2.5	−5.98	−8.25 ± 0.19	−2.27		
DHF binding to DHFR·$NADP^+$	H_2O	2.59 ± 0.07	−7.62	−10.4 ± 0.04	−2.77	0.74 ± 0.01	−1.18
DHF binding to DHFR·$NADP^+$	D_2O	2.59 ± 0.06	−7.62	−9.21 ± 0.04	−1.59	0.75 ± 0.01	

[a]Molar enthalpies for binding of NADPH to the apoenzyme were obtained using the first few points from subsaturating ITC titrations. At least two data sets for binding of DHF to the enzyme·$NADP^+$ complex were analyzed by global fitting to a single-site model (A + B ↔ AB) in SEDPHAT.[36] For folate binding to the apoenzyme, global fits to a two-site model (A + B + B ↔ AB +B ↔ ABB) giving macroscopic binding constants were used. The Gibbs free energy values were calculated from the equation $\Delta G = -RT \ln K_d$, and $T\Delta S$ values were obtained from the relationship $\Delta G = \Delta H - T\Delta S$.

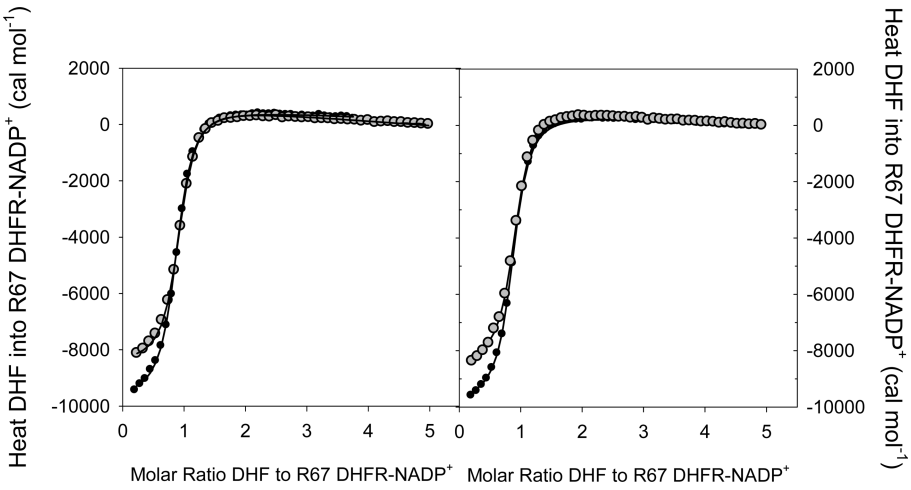

Figure 6. Comparison of the DHF titrations into the R67 DHFR·$NADP^+$ complex in water and D_2O-based buffers. The D_2O data are colored gray, while the H_2O data are colored black. The enzyme concentration was 100 μM, and the $NADP^+$ concentration was 500 μM. The DHF syringe concentrations ranged from 3.6 to 4.3 mM. To reach equilibrium, 4 min was allowed between each injection. Each data set was first opened using Origin version 7, and the first two points were removed. Next, two different titrations were imported into SEDPHAT version 8.2[36] and globally fit to a single-site model. The fits from the SEDPHAT analysis are listed in Table 2.

However, in our hands, PPC is not statistically robust enough for the calculation of the number of waters released upon binding of DHF to R67 DHFR.

ITC in H_2O versus D_2O. To explore the contribution of water reorganization to ligand binding, we used the approach of Chervenak and Toone[16] and monitored binding in the presence of D_2O. Here, the difference in H acceptor to D acceptor interaction enthalpies helps estimate the contribution of solvent reorganization during binding. Chervenak and Toone state, "To a first approximation, $\Delta\Delta H$ (=$\Delta H_{H_2O} - \Delta H_{D_2O}$) represents 10% of the contribution of changes in solvation to the enthalpy of binding." An assumption of this treatment is that the structures of the ligand, protein, and complex are identical in both solvents.

Binding of NADPH to the apoenzyme was monitored in aqueous TE buffer as well as a D_2O-based buffer. A comparison of the total heat plots (where the data are not fit to a model) shows duplicate titrations overlap reasonably well; further, a more negative enthalpy is associated with binding in D_2O compared to H_2O (see Figure S5 of the Supporting Information). The data were fit to both single- and two-site models using SEDPHAT. For the two-symmetric site model, K_d values for the first site (3−4 μM, microscopic values) indicated saturation was easily achieved; however, values for the second site indicate much weaker binding (~0.7 mM, microscopic values), consistent with the second site not being fully saturated. This results in a low c value for the second site and limits our confidence in the overall fit as the values are linked. Fitting the data to a single-site model is also problematic as all the data are forced into a single value. Therefore, we turned to measuring binding of NADPH to the first site by injecting very low concentrations of cofactor; these are conditions at which all ligand should bind, which allows a model-independent measurement of molar enthalpy.[33] This approach yields enthalpy values that are within error of each other for binding in H_2O and D_2O (see Table 2). We therefore conclude that water reorganization does not contribute to the

dx.doi.org/10.1021/bi301544k | Biochemistry 2013, 52, 2118−2127

enthalpy associated with the physiologically relevant binding of the first NADPH molecule.

Next, binding of folate to the apoenzyme was monitored, and as previously observed, two folate molecules bind with positive cooperativity.[19] Figure S6 of the Supporting Information shows the global fitting of two titrations performed in D_2O compared to those for the water titrations. While the K_d and ΔG values are quite close, there are more obvious changes in the ΔH terms. Binding to the first site is driven by enthalpy and entropy, while binding to the second site is driven by enthalpy. The $\Delta\Delta H$ ($\Delta H_{H_2O} - \Delta H_{D_2O}$) for the first site is 2.7 kcal/mol, while that for the second site is −1.06 kcal/mol. The enthalpy of a hydrogen bond is 10% greater in D_2O than in H_2O.[16,44−46] As the change in signal is one-tenth of the total enthalpy of solvent replacement, any changes in ΔH_{obs} due to $\Delta H_{solvent}$ are 10 times the $\Delta\Delta H$. For the case of the first binding site of folate, a value 10 times the $\Delta\Delta H$ is 10-fold greater than the observed binding enthalpy. This discrepancy likely means that the structure of the ligand, protein, and/or complex is not the same in both solvents. Because the fit values are coupled, we cannot accurately determine the effect of D_2O on the second site. Also of interest, while most previous ITC studies find less negative ΔH values in D_2O than in H_2O, some groups[47,48] have obtained more negative values as observed here for the first folate binding event.

Finally, formation of the R67 DHFR·DHF·$NADP^+$ complex was monitored by addition of DHF to the enzyme·$NADP^+$ complex (1:5 ratio). The data are shown in Figure 6, and as noted in Table 2, a less negative enthalpic signal was observed in D_2O compared to H_2O. The $\Delta\Delta H$ value is −1.18 kcal/mol. If a value 10 times the $\Delta\Delta H$ difference provides a first approximation of the contribution of solvent reorganization to the observed enthalpy, then this value is −11.8 kcal/mol. While this is slightly higher (i.e., 114%) than the total signal observed in water, it suggests that water reorganization is the dominant, if not entire, contributor to this enthalpic signal.

DISCUSSION

A model for binding of DHF to any DHFR is given in Figure 1. The first row in the model proposes that water release occurs upon binding of DHF to either R67 DHFR or the nonhomologous *E. coli* chromosomal DHFR (EcDHFR). This view is supported by accessible surface area (ASA) calculations (see the Supporting Information) and by our present HHP measurements on R67 DHFR along with the Gekko lab's HHP results on EcDHFR.[31] The second part of the model hypothesizes that osmolytes interact weakly with folate·DHF and that dissociation of the osmolyte is required prior to binding of DHF/folate to the enzyme active site. This proposal is supported by our osmotic pressure (OP) studies of R67 DHFR and EcDHFR in which both enzymes show weaker DHF binding in the presence of added osmolytes.[10,14] NMR studies also indicate that osmolytes interact with free folate in solution.[15]

Effects of Pressure on Cofactor Binding. R67 DHFR is reasonably refractory to increasing pressure, as it maintains full activity until the pressure reaches ∼200 MPa. However, cofactor binding is affected as increasing HHP weakens the ability of R67 DHFR to bind NADPH (Figure 4). This result is consistent with a disfavored, larger volume of the enzyme··NADPH complex compared to that of the free enzyme and free ligand. It is also consistent with an increased level of hydration of NADPH at higher pressures, which negatively affects complexation. These data also agree with the R67 DHFR·$NADP^+$ crystal structure in which the cofactor displays numerable contacts with the enzyme.[17]

Role of Water in Substrate Binding. HHP effects on DHF capture were monitored using progress curves and the integrated Michaelis−Menten equation. As the effect of HHP on k_{cat} (−19.4 ± 2.0 cm^3/mol) is smaller than the effect on $1/K_{m(DHF)}$ (22.8 ± 2.3 cm^3/mol), the net effect on $k_{cat}/K_{m(DHF)}$ yields a positive activation volume of 3.3 ± 0.5 cm^3/mol (Figure 5). As the activation volume for k_{cat} is substantial, it may be that $1/K_m$ more accurately measures substrate capture than k_{cat}/K_m. However, both volumes containing information about substrate capture are positive, denoting increased pressure disfavors this process. Again, we note that at ambient pressure, $K_{m(DHF)}$ equals $K_{d(DHF)}$ as measured by ITC.[10,40]

The calculated volume of association of NADPH to R67 DHFR is 11.4 ± 0.5 cm^3/mol. While this volume as well as the volume for substrate capture may not describe "real space",[5] they are both positive, indicating an increased pressure disfavors both NADPH binding and DHF capture. We also note the activation volumes for k_{cat} in EcDHFR and R67 DHFR are different; this likely arises from their use of exo and endo transition states,[49] respectively.

What Is the Origin of the Enthalpy Observed upon DHF Binding? This question is of interest for two reasons. First, the pABA-Glu tail of DHF/folate is disordered in the R67 DHFR structure from NMR[50] and X-ray structural data[17,23] as well as molecular dynamics.[51] Second, given this disorder, it is surprising that a semilog plot of the observed enthalpy for folate binding to the R67 DHFR·NADPH complex versus $k_{cat}/K_{m(DHF)}$ shows a linear correlation over a 200−250-fold range of rates and an 8 kcal·mol^{-1} difference in ΔH for the wild type and six mutant R67 DHFRs as well as the use of the alternate cofactor, NADH.[20] [Note a similar linear correlation is seen when the ΔH for DHF binding to the R67 DHFR·$NADP^+$ complex is compared to log $k_{cat}/K_{m(DHF)}$.[52]]

Our original hypothesis for explaining the linear correlation between the ΔH for ground state folate/DHF binding and log $k_{cat}/K_{m(DHF)}$ suggested the importance of interactions between R67 and DHF, focusing on interactions with the pteridine ring at the center of the active site pore. Use of DHF fragments allowed evaluation of this hypothesis. When binding of dihydropteroate (DHP, which has the Glu tail removed) is considered, 40% of the enthalpic signal is lost, yet the K_d is weakened only to 25 μM.[53] Further truncation of the pABA-Glu tail to dihydrobiopterin (DHB, pteridine ring with a CH_2OH-CH_2OH-CH_3 tail off the C6 atom) results in the loss of the ITC signal, yet DHB still binds, with a K_i of 160 μM.[53] Because removal of the disordered tail results in progressive loss of the enthalpic signal, these surprising results led us to consider how the pABA-Glu tail might contribute to ΔH. Analysis of the R67·DHF·$NADP^+$ crystal structure[17] and MD simulations[51] suggest formation of solvent-separated ion pairs as well as direct ion pairs between the α- and γ-carboxylates of the Glu tail of DHF with the two symmetry-related K32 residues at the edge of the active site pore (see the bottom panel of Figure 2). Also, our previous ITC studies of folate binding to the R67 DHFR·NADPH complex in the presence of increasing concentrations of NaCl (ionic strength range of 0.032−0.32) found a titration in enthalpy (from −13000 to −5800 kcal/mol), but no change in K_d.[40]

dx.doi.org/10.1021/bi301544k | *Biochemistry* 2013, 52, 2118−2127

To test the role of K32 in DHF binding, we previously constructed a K32M/1+3 double mutant using a tandem array of four fused R67 DHFR genes. In this construct, the K32 residues were replaced by methionine in one half of the active site pore, blocking ion pair formation (see Figure 2). The K_m for DHF increased by at least 60-fold; however, protein stability problems made it difficult to characterize this mutant using ITC. As Q67H mutations tighten binding to both NADPH and DHF by stacking with the pterin and nicotinamide rings,[54] four additional Q67H mutations were added to the K32M/1+3 mutant in our quadruplicated gene product.[55] Tighter binding of DHF results, indicating the K32 residue is sufficient but not necessary for DHF binding. Surprisingly, the Q67H/1+2+3+4 and K32M/1+3 multimutant displays a more negative enthalpic signal than the quadruplicated gene product upon ternary DHF complex formation, indicating formation of an ion pair between the pABA-Glu tail and K32 does not dominate the ΔH signal. (A discussion and Table S1 concerning an alternate possibility that loss of any contribution to the ΔH signal from ion pair formation is compensated by addition of interactions due to the Q67H mutations are provided in the Supporting Information.)

While compensating effects may be involved in the experiments described above, neither contacts of the pteridine ring with the R67·NADPH complex nor formation of an ion pair between the Glu tail of DHF and K32 residues appear to dominate the enthalpic signature for ternary DHF complex formation. What remains is water reorganization.

In this study, we compare binding in H_2O versus D_2O to examine the role of water reorganization in ligand binding.[16,47] From Table 2 and Figure 6, we observe a less negative enthalpy associated with ternary DHF complex formation in D_2O. Because the ΔG values in both H_2O and D_2O are similar, the $\Delta\Delta H$ value suggests the bound state is less rigid in D_2O. Using the assumption that the H-acceptor bond energy is 10% smaller than that of the D-acceptor bond,[16] a value that is 10 times $\Delta\Delta H$ of −11.8 can be approximated. This value corresponds to roughly 110% of the overall signal, indicating that solvent reorganization either dominates or fully describes the enthalpy term in ternary complex formation.

Solvent reorganization may encompass dewetting of hydrophobic surfaces[56] and dipole reorientation around ionized residues,[57] as well as alterations in H-bonding networks of solvation shells.[58] In addition, numerous proposals suggest two different types of water, e.g., disordered and more dense water versus more ordered, icelike, and less dense water.[59−64] Switching between these two phases may occur. Recent force microscopy studies find that water molecules confined between two hydrophilic surfaces that are ≤20 Å apart are much more viscous than bulk water.[65−67] Accompanying MD studies proposed this phenomenon arose from an increased number of hydrogen bonds to the surfaces. Further, a recent computational study by Baron et al.[68] finds that water can be an active player in idealized ligand−cavity interactions. In particular, ion pair formation results in enthalpy-driven binding, with a large contribution from the enthalpy due to formation of new water−water interactions upon desolvation (see Figure 4 of ref 68).

Finally, it seems likely that the hydrophobic and aromatic moieties in folate/DHF affect the water structure in its hydration shell. Calculation of logP from the LigX option in MOE version 2009.10 (Chemical Computing Group) predicts NADPH to be less hydrophobic than DHF/folate with logP values of −7.774 and −3.875, respectively. These values indicate folate is much more hydrophobic than the cofactor and, as such, may show more effects on water behavior. This is consistent with our observation that binding of the cofactor to its first tight site does not show altered enthalpies while folate/DHF binding does indicate solvent reorganization effects.

CONCLUSION

We find that water is quite important in binding of DHF to R67 DHFR. Water appears to be released upon binding based on our ΔASA calculations and our HHP studies. Additionally, water reorganization appears to be important from our ITC studies comparing binding of DHF to the enzyme·$NADP^+$ complex in H_2O versus D_2O. Here, solvent reorganization upon ternary complex formation either dominates or wholly captures the enthalpy value. In short, water appears to play an active, rather than a passive, role[61,62,67,69] in DHF ternary complex formation.

ASSOCIATED CONTENT

Supporting Information

A graph of ln k_{cat} versus pressure, a plot showing the reversibility of the R67 DHFR reaction with respect to pressure, a sample progress curve analysis at 175 MPa, a plot and discussion of steady state rate analysis of HHP effects on the R67 DHFR Y69L mutant, the total heat plots from ITC experiments describing binding of NADPH to R67 DHFR, a comparison of the ITC titrations of folate into apo R67 DHFR in water and D_2O-based buffers, a discussion and table of enthalpy effects for various mutant DHFRs, accessible surface area calculations, and a pressure perturbation calorimetry section that includes materials and methods, a sample titration, a results section, a table of results, and the code for a SAS program used for bootstrap analysis are provided. This material is available free of charge via the Internet at http://pubs.acs.org.

AUTHOR INFORMATION

Corresponding Author

*Department of Biochemistry and Cellular and Molecular Biology, University of Tennessee, Knoxville, TN 37996-0840. Phone: (865) 974-4507. Fax: (865) 974-6306. E-mail: lzh@utk.edu.

Funding

This work was supported by National Science Foundation Grant MCB-0817827.

Notes

The authors declare no competing financial interest.

ACKNOWLEDGMENTS

We thank Harini Patel, Katie Kelley, and Jordan Grubbs for their help in protein purification. We thank Shelley Jones for help with the HHP instrumentation. We also thank Dr. Kunihiko Gekko for supplying us with the MATLAB program used for progress curves analysis.

ABBREVIATIONS

ASA, accessible surface area; DHF, dihydrofolate; EcDHFR, chromosomal DHFR from *E. coli*; HHP, high hydrostatic pressure; MTA buffer, 100 mM Tris, 50 mM MES, 50 mM acetic acid buffer; $NADP^+$ and NADPH, oxidized and reduced nicotinamide adenine dinucleotide phosphate, respectively; OP, osmotic pressure; R67 DHFR, R67 dihydrofolate reductase; TE, 10 mM Tris and 1 mM EDTA buffer (pH 7.5) with 102

mM NaCl; TMP, trimethoprim; wt, wild-type; Y69L, tyrosine 69 to leucine R67 DHFR mutant.

■ ADDITIONAL NOTE

[a]The data in Figure 2 indicate a much smaller effect of HHP on k_{cat}. However, it may be that the levels of DHF used in those experiments were not sufficiently high to be saturating at high pressures. While 70−120 μM DHF would be saturating at ambient pressure, our progress curve analysis suggests a large effect of pressure on DHF capture.

■ REFERENCES

(1) Whitesides, G. M., and Krishnamurthy, V. M. (2005) Designing ligands to bind proteins. *Q. Rev. Biophys. 38*, 385−395.

(2) Munos, B. (2009) Lessons from 60 years of pharmaceutical innovation. *Nat. Rev. Drug Discovery 8*, 959−968.

(3) Petsko, G. A. (2010) When failure should be the option. *BMC Biol. 8*, 61−64.

(4) Silva, J. L., Foguel, D., and Royer, C. A. (2001) Pressure provides new insights into protein folding, dynamics and structure. *Trends Biochem. Sci. 26*, 612−618.

(5) Northrop, D. B. (2006) Unusual origins of isotope effects in enzyme-catalysed reactions. *Philos. Trans. R. Soc., B 361*, 1341−1349.

(6) Robinson, C. R., and Sligar, S. G. (1995) Hydrostatic and osmotic pressure as tools to study macromolecular recognition. *Methods Enzymol. 259*, 395−427.

(7) Kornblatt, J. A., and Kornblatt, M. J. (2002) The effects of osmotic and hydrostatic pressures on macromolecular systems. *Biochim. Biophys. Acta 1595*, 30−47.

(8) Kornblatt, J. A., and Kornblatt, M. J. (2002) Water as it applies to the function of enzymes. *Int. Rev. Cytol. 215*, 49−73.

(9) Robinson, C. R., and Sligar, S. G. (1994) Hydrostatic pressure reverses osmotic pressure effects on the specificity of EcoRI-DNA interactions. *Biochemistry 33*, 3787−3793.

(10) Chopra, S., Dooling, R., Horner, C. G., and Howell, E. E. (2008) A balancing act: Net uptake of water during dihydrofolate binding and net release of water upon NADPH binding in R67 dihydrofolate reductase. *J. Biol. Chem. 283*, 4690−4698.

(11) Fried, M. G., Stickle, D. F., Smirnakis, K. V., Adams, C., MacDonald, D., and Lu, P. (2002) Role of hydration in the binding of lac repressor to DNA. *J. Biol. Chem. 277*, 50676−50682.

(12) LiCata, V. J., and Allewell, N. M. (1997) Functionally linked hydration changes in *Escherichia coli* aspartate transcarbamylase and its catalytic subunit. *Biochemistry 36*, 10161−10167.

(13) Reid, C., and Rand, R. P. (1997) Probing protein hydration and conformational states in solution. *Biophys. J. 72*, 1022−1030.

(14) Grubbs, J., Rahmanian, S., Deluca, A., Padmashali, C., Jackson, M., Duff, M. R., and Howell, E. E. (2011) Thermodynamics and solvent effects on substrate and cofactor binding in *Escherichia coli* chromosomal dihydrofolate reductase. *Biochemistry 50*, 3673−3685.

(15) Duff, M. R., Jr., Grubbs, J., Serpersu, E., and Howell, E. E. (2012) Weak interactions between folate and osmolytes in solution. *Biochemistry 51*, 2309−2318.

(16) Chervenak, M. C., and Toone, E. J. (1994) A direct measure of the contribution of solvent reorganization to the enthalpy of binding. *J. Am. Chem. Soc. 116*, 10533−10539.

(17) Krahn, J., Jackson, M., DeRose, E. F., Howell, E. E., and London, R. E. (2007) Structure of a type II dihydrofolate reductase ternary complex: Use of identical binding sites for unrelated ligands. *Biochemistry 46*, 14878−14888.

(18) Howell, E. E. (2005) Searching sequence space: Two different approaches to dihydrofolate reductase catalysis. *ChemBioChem 6*, 590−600.

(19) Bradrick, T. D., Beechem, J. M., and Howell, E. E. (1996) Unusual binding stoichiometries and cooperativity are observed during binary and ternary complex formation in the single active pore of R67 dihydrofolate reductase, a D_2 symmetric protein. *Biochemistry 35*, 11414−11424.

(20) Strader, M. B., Chopra, S., Jackson, M., Smiley, R. D., Stinnett, L., Wu, J., and Howell, E. E. (2004) Defining the binding site of homotetrameric R67 dihydrofolate reductase and correlating binding enthalpy with catalysis. *Biochemistry 43*, 7403−7412.

(21) Amyes, S. G., and Smith, J. T. (1976) The purification and properties of the trimethoprim-resistant dihydrofolate reductase mediated by the R-factor, R388. *Eur. J. Biochem. 61*, 597−603.

(22) Stone, D., and Smith, S. L. (1979) The amino acid sequence of the trimethoprim-resistant dihydrofolate reductase specified in *Escherichia coli* by R-plasmid R67. *J. Biol. Chem. 254*, 10857−10861.

(23) Narayana, N., Matthews, D. A., Howell, E. E., and Nguyen-huu, X. (1995) A plasmid-encoded dihydrofolate reductase from trimethoprim-resistant bacteria has a novel D2-symmetric active site. *Nat. Struct. Biol. 2*, 1018−1025.

(24) Reece, L. J., Nichols, R., Ogden, R. C., and Howell, E. E. (1991) Construction of a synthetic gene for an R-plasmid-encoded dihydrofolate reductase and studies on the role of the N-terminus in the protein. *Biochemistry 30*, 10895−10904.

(25) Eisenmenger, M. J., and Reyes-De-Corcuera, J. I. (2009) High hydrostatic pressure increased stability and activity of immobilized lipase in hexane. *Enzyme Microb. Technol. 45*, 118−125.

(26) Quinlan, R. J., and Reinhart, G. D. (2005) Baroresistant buffer mixtures for biochemical analyses. *Anal. Biochem. 341*, 69−76.

(27) Dunn, S. M., Lanigan, T. M., and Howell, E. E. (1990) Dihydrofolate reductase from *Escherichia coli*: Probing the role of aspartate-27 and phenylalanine-137 in enzyme conformation and the binding of NADPH. *Biochemistry 29*, 8569−8576.

(28) Blakley, R. L. (1960) Crystalline dihydropteroylglutamic acid. *Nature 188*, 231−232.

(29) Horecker, B. L., and Kornberg, A. (1948) The extinction coefficients of the reduced band of pyridine nucleotides. *J. Biol. Chem. 175*, 385−390.

(30) Baccanari, D., Phillips, A., Smith, S., Sinski, D., and Burchall, J. (1975) Purification and properties of *Escherichia coli* dihydrofolate reductase. *Biochemistry 14*, 5267−5273.

(31) Ohmae, E., Tatsuta, M., Abe, F., Kato, C., Tanaka, N., Kunugi, S., and Gekko, K. (2008) Effects of pressure on enzyme function in *Esherichia coli* dihydrofolate reductase. *Biochim. Biophys. Acta 1784*, 1115−1121.

(32) Wiseman, T., Williston, S., Brandts, J. F., and Lin, L. N. (1989) Rapid measurement of binding constants and heats of binding using a new titration calorimeter. *Anal. Biochem. 179*, 131−137.

(33) Hutchins, R. A., Crenshaw, J. M., Graves, D. E., and Denny, W. A. (2003) Influence of substituent modifications on DNA binding energetics of acridine-based anticancer agents. *Biochemistry 42*, 13754−13761.

(34) Cook, P. (1991) *Enzyme Mechanism from Isotope Effect*, CRC Press, Boca Raton, FL.

(35) Quinn, D. M., and Sutton, L. D. (2000) Theoretical basis and mechanistic utility of solvent isotope effects. In *Enzyme Mechanism from Isotope Effects* (Cook, P., Ed.) pp 73−126, CRC Press, Boca Raton, FL.

(36) Houtman, J. C., Brown, P. H., Bowden, B., Yamaguchi, H., Appella, E., Samelson, L. E., and Schuck, P. (2007) Studying multisite binary and ternary protein interactions by global analysis of isothermal titration calorimetry data in SEDPHAT: Application to adaptor protein complexes in cell signaling. *Protein Sci. 16*, 30−42.

(37) Herve, G., Tobe, S., Heams, T., Vergne, J., and Maurel, M. C. (2006) Hydrostatic and osmotic pressure study of the hairpin ribozyme. *Biochim. Biophys. Acta 1764*, 573−577.

(38) Hay, S., Sutcliffe, M. J., and Scrutton, N. S. (2007) Promoting motions in enzyme catalysis probed by pressure studies of kinetic isotope effects. *Proc. Natl. Acad. Sci. U.S.A. 104*, 507−512.

(39) Tobe, S., Heams, T., Vergne, J., Herve, G., and Maurel, M. C. (2005) The catalytic mechanism of hairpin ribozyme studied by hydrostatic pressure. *Nucleic Acids Res. 33*, 2557−2564.

(40) Hicks, S. N., Smiley, R. D., Hamilton, J. B., and Howell, E. E. (2003) Role of ionic interactions in ligand binding and catalysis of R67 dihydrofolate reductase. *Biochemistry 42*, 10569−10578.

(41) Lin, L. N., Brandts, J. F., Brandts, J. M., and Plotnikov, V. (2002) Determination of the volumetric properties of proteins and other solutes using pressure perturbation calorimetry. *Anal. Biochem. 302*, 144−160.
(42) Cooper, A., Johnson, C. M., Lakey, J. H., and Nollmann, M. (2001) Heat does not come in different colours: Entropy-enthalpy compensation, free energy windows, quantum confinement, pressure perturbation calorimetry, solvation and the multiple causes of heat capacity effects in biomolecular interactions. *Biophys. Chem. 93*, 215−230.
(43) Cameron, D. L., Jakus, J., Pauleta, S. R., Pettigrew, G. W., and Cooper, A. (2010) Pressure perturbation calorimetry and the thermodynamics of noncovalent interactions in water: Comparison of protein-protein, protein-ligand, and cyclodextrin-adamantane complexes. *J. Phys. Chem. B 114*, 16228−16235.
(44) Marcus, Y., and Ben-Naim, A. (1985) A study of the structure of water and its dependence on solutes, based on the isotope effects on solvation thermodynamics in water. *J. Chem. Phys. 83*, 4744−4759.
(45) Muller, N. (1991) Model-calculations of changes of thermodynamic variables for the transfer of nonpolar solutes from water to water-D2. *J. Solution Chem. 20*, 669−680.
(46) Nemethy, G., and Scheraga, H. A. (1964) Structure of water + hydrophobic bonding in proteins. 4. Thermodynamic properties of liquid deuterium oxide. *J. Chem. Phys. 41*, 680−689.
(47) Ozen, C., Norris, A. L., Land, M. L., Tjioe, E., and Serpersu, E. H. (2008) Detection of specific solvent rearrangement regions of an enzyme: NMR and ITC studies with aminoglycoside phosphotransferase(3′)-IIIa. *Biochemistry 47*, 40−49.
(48) Sobhany, M., Dong, J., and Negishi, M. (2005) Two-step mechanism that determines the donor binding specificity of human UDP-N-acetylhexosaminyltransferase. *J. Biol. Chem. 280*, 23441−23445.
(49) Castillo, R., Andres, J., and Moliner, V. (1999) Catalytic mechanism of dihydrofolate reductase enzyme. A combined quantum-mechanical/molecular-mechanical characterizaton of transition state structure for the hydride transfer step. *J. Am. Chem. Soc. 121*, 12140−12147.
(50) Li, D., Levy, L. A., Gabel, S. A., Lebetkin, M. S., DeRose, E. F., Wall, M. J., Howell, E. E., and London, R. E. (2001) Interligand Overhauser effects in type II dihydrofolate reductase. *Biochemistry 40*, 4242−4252.
(51) Kamath, G., Howell, E. E., and Agarwal, P. K. (2010) The tail wagging the dog: Insights into catalysis in R67 dihydrofolate reductase. *Biochemistry 49*, 9078−9088.
(52) Strader, M. B. (2003) Identifying the catalytic and ligand binding roles of active site residues in homotetrameric R67 dihydrofolate reductase. Ph.D. Thesis, University of Tennessee, Knoxville, TN.
(53) Jackson, M., Chopra, S., Smiley, R. D., Maynord, P. O., Rosowsky, A., London, R. E., Levy, L., Kalman, T. I., and Howell, E. E. (2005) Calorimetric studies of ligand binding in R67 dihydrofolate reductase. *Biochemistry 44*, 12420−12433.
(54) Divya, N., Grifith, E., and Narayana, N. (2007) Structure of the Q67H mutant of R67 dihydrofolate reductase-$NADP^+$ complex reveals a novel cofactor binding mode. *Protein Sci. 16*, 1063−1068.
(55) Feng, J., Goswami, S., and Howell, E. E. (2008) R67, the other dihydrofolate reductase: Rational design of an alternate active site configuration. *Biochemistry 47*, 555−565.
(56) Chandler, D. (2005) Interfaces and the driving force of hydrophobic assembly. *Nature 437*, 640−647.
(57) LeBard, D. N., and Matyushova, D. V. (2008) Redox entropy of plastocyanin: Developing a microscopic view of mesoscopic polar solvation. *J. Chem. Phys. 128*, 155106−155116.
(58) Gilman-Politi, R., and Harries, D. (2011) Unraveling the Molecular Mechanism of Enthalpy Driven Peptide Folding by Polyol Osmolytes. *J. Chem. Theory Comput. 7*, 3816−3828.
(59) Muller, N. (1990) Search for a realistic view of hydrophobic effects. *Acc. Chem. Res. 23*, 23−28.
(60) Tanaka, H. (2000) General view of a liquid-liquid phase transition. *Phys. Rev. E: Stat. Phys., Plasmas, Fluids, Relat. Interdiscip. Top. 62*, 6968−6976.
(61) Ball, P. (2008) Water: An enduring mystery. *Nature 452*, 291−292.
(62) Ball, P. (2008) Water as an active constituent in cell biology. *Chem. Rev. 108*, 74−108.
(63) Huang, C., Wikfeldt, K. T., Tokushima, T., Nordlund, D., Harada, Y., Bergmann, U., Niebuhr, M., Weiss, T. M., Horikawa, Y., Leetmaa, M., Ljungberg, M. P., Takahashi, O., Lenz, A., Ojamae, L., Lyubartsev, A. P., Shin, S., Pettersson, L. G., and Nilsson, A. (2009) The inhomogeneous structure of water at ambient conditions. *Proc. Natl. Acad. Sci. U.S.A. 106*, 15214−15218.
(64) Mallamace, F. (2009) The liquid water polymorphism. *Proc. Natl. Acad. Sci. U.S.A. 106*, 15097−15098.
(65) Major, R. C., Houston, J. E., McGrath, M. J., Siepmann, J. I., and Zhu, X.-Y. (2006) Viscous Water Meniscus under Nanoconfinement. *Phys. Rev. Lett. 96*, 177803.
(66) Li, T.-D., Gao, J., Szoszkiewicz, R., Landman, U., and Riedo, E. (2007) Structured and viscous water in sub-nanometer gaps. *Phys. Rev. B 75*, 115415.
(67) Ball, P. (2008) Water as a biomolecule. *ChemPhysChem 9*, 2677−2685.
(68) Baron, R., Setny, P., and McCammon, J. A. (2010) Water in cavity-ligand recognition. *J. Am. Chem. Soc. 132*, 12091−12097.
(69) Biela, A., Nasief, N. N., Betz, M., Heine, A., Hangauer, D., and Klebe, G. (2013) Dissecting the hydrophobic effect on the molecular level: The role of water, enthalpy, and entropy in ligand binding to thermolysin. *Angew. Chem., Int. Ed. 52*, 1822−1828.